UNCONVENTIONAL RESOURCES TECHNOLOGY CONFERENCE
FUELED BY SPE • AAPG • SEG

URTeC: 3865660

Rock Thin-section Analysis and Mineral Detection Utilizing Deep Learning Approach

Fatick Nath*[1], Sarker Asish[2], Shaon Sutradhar[3], Zhiyang Li[1], Nazmul Shahadat[2], Happy R Debi[2], S M Shamsul Hoque[4] , 1. School of Engineering, Texas A&M International University, Laredo, TX, United States, 2. School of Computing & Informatics, University of Louisiana at Lafayette, Lafayette, LA, United States, 3. University of A Coruña, Spain, 4. School of Geosciences, University of Louisiana at Lafayette, LA, United States

This paper was prepared for presentation at the Unconventional Resources Technology Conference held in Denver, Colorado, USA, 13-15 June 2023.

Abstract

Rock thin-section identification is crucial in understanding the sedimentary environment of the reservoir, formulating the oil and gas development plan, distinguishing reservoir space and pore structure, and identifying the petrological characteristics of reservoirs. However, the traditional thin-section identification method is subject to strong subjectivity, high reliance on experience, heavy workload, long identification cycle, and inability to achieve complete and accurate quantification. This article uses generalized, robust, and parameter-efficient deep-learning architectures for mineral identification and characterization to fill the gap.

This study covers a total of 4 classes (quartz, feldspar, calcite, and matrix) of 993 representative images in a clastic sedimentary rock, Mancos shale. The proposed architecture for automated classification is divided into the following stages: (1) input microscopic thin-section images and augmentation, (2) perform segmentation, (3) identify and classify mineral types, (4) observation and identification of particles. The total 993 thin-section images were split into the ratio of 8:2 for model training and testing. This study utilized a U-net deep learning architecture for classifying four classes.

The results demonstrated that the current deep-learning models perform superior to the baseline models for image segmentation, minerals identification, and classification. The overall accuracy with more than 91% shows that the model is very confident for detecting the 4 classes (quartz, feldspar, calcite, and matrix) are defined. It was evident that the particle segmentation network based on the proposed model is higher than the baseline models.

This study presents a reliable method for identifying thin sections of Mancos shale that has the potential to increase identification accuracy and decrease the influence of subjectivity from the human observer. While the traditional identification method depends on visual observation, adopting deep learning based intelligent identification can significantly aid the process of quantitative extraction of information efficiently with higher accuracy. Therefore, this approach used in this paper provides more comprehensive, quantitative, and accurate information for the microscopic thin-section images.

Introduction

Classifying rocks is necessary for geological engineering, rock physics, mining engineering, and finding resources. The external characteristics of rocks are influenced by various factors such as lighting, shading, humidity, and shape. The primary technique for recognizing distinct features on rocks in situ is using a magnifying lens and a knife. Rock thin-section photographs exhibit color, grain size, form, internal cleavage, structure, and other characteristics as a result of the mineral compositions of the rocks (Li et al. 2022). These characteristics provide insight about the petrographic characteristics of rocks.

To identify each characteristic and based on the found features, to categorize a rock thin-section image, it requires highly skilled geologist. Moreover, this manual process is very time expensive, tedious and financially expensive. On the other hand, the modern computer scient has advanced significantly that such manual inspection of thin-sections photographs can be performed in fully automatic procedure with meticulous consistency compared to manual process using the application of computer vision and deep learning technologies.

Techniques to identify different properties and classifying an image include classical image processing using pixel-wise, local filtering and morphological operations, statistical and feature engineering-based machine learning approaches and modern deep learning techniques. In the work of Jobe et al. (2018), sophisticated image analysis and machine learning algorithms were applied to detect geological features from thin-section photographs. Abedini et al. (2018) exploited two novel machine learning models, one using shallow learning and one using deep learning, for identifying porosity types in thin sections. Rubo et al. (2019) approached classical artificial neural networks and random forest classifiers-based model for detecting mineralogy and porosity in petrographic thin slices of carbonate rocks.

In the work of Xu et al. (2020), state-of-the-art visual recognition model ResNet-18 was trained from scratch to classify four types of rock thin sections. In a similar objective, Nanjo et al. (2019) implemented convolutional neural network-based model to classify four types of rock components. Cheng et al. (2013) implemented ensemble model that takes three different input image modalities and performed classification of rock into 13 classes. Nanjo et al. demonstrated deep convolutional neural network-based model for carbonate rock lithology recognition. Among these works, machine learning and deep learning-based models showed superior performance and easier operation for users, however, preparation of the training dataset was time and energy extensive work.

Object segmentation techniques are applied to identify and classify objects at pixel-level in images. Traditional image processing techniques for object segmentation are complex and inefficient, however, widely exploited, until deep learning based semantic segmentations models, e.g., U-Net (Ronneberger et al., 2015) and its different variants, e.g., U-Net++ (Zhou et al. 2018), ResU-Net (Zhang et al., 2018), etc. were recently introduced. Segmenting rock particles and determining their edge contour using image processing and/or deep learning algorithms enables automatic thin-section identification and quantitative compaction assessment (Budennyy et al., 2017; Buono, 2019; Pattnaik et al., 2020a; Pattnaik et al., 2020b).

Past researchers used different techniques for identifying and classifying the thin section images. Hu et al. (2012) created a sequence image analysis system for rock-thin sections based on continuous extinction feature analysis under orthogonal polarization. The edges of pores can be retrieved using image processing techniques, and multiple studies have described simple throat identification methods (Ma and Gao, 2017). Using orthogonal polarization sequence pictures, Zhang et al. connected pixel scale to extinction angle (Zhang et al., 2020).

In summary, the existing literature on intelligent thin-section identifications primarily concentrates on specific tasks such as particle segmentation and pore extraction, lacking comprehensive and methodical coverage of the subject matter. Furthermore, the employed research methodologies typically rely on image processing technology, yet they fail to incorporate the geological expertise of specialists in rock/mineral identification. In addition, the field of core analysis, which includes mineral composition identification,

pore structure analysis, and rock structure analysis, has yet to fully complete the identification of intelligent thin sections. Although the thin-section identification has been helpful, it is not yet possible to say with certainty that it constitutes a comprehensive quantitative evaluation. Intelligent thin-section identification that is both scientifically rigorous and quantitatively precise requires the creation of a deep-learning algorithm that can integrate data on geological facies.

This work analyzes automatic mineral identification and classification by employing generalized, robust, and parameter-efficient deep-learning architectures. The objectives of this work are - i) prepare a dataset with annotated ground-truths with calcite, quartz, and chlorite objects in thin-section images, ii) pixel-wise classification of calcite, quartz, and chlorite minerals by geological facies and depth from thin-section images of Mancos shale using deep learning based supervised model that requires minimal effort to train and test.

Methodology

This work proposes a supervised semantic segmentation method using U-Net for pixel-wise identification of rock mineral constitutes from thin-section images. First, we collect raw thin-section images. Afterwards, we annotate images. After annotating, we patchify the images and randomly distribute patches for model training, validation and testing. Then we train the model with U-Net model. Finally, during inference, we test our model and evaluate the model performance on test dataset. A pictorial overview of our proposed methodology is given in Figure 1.

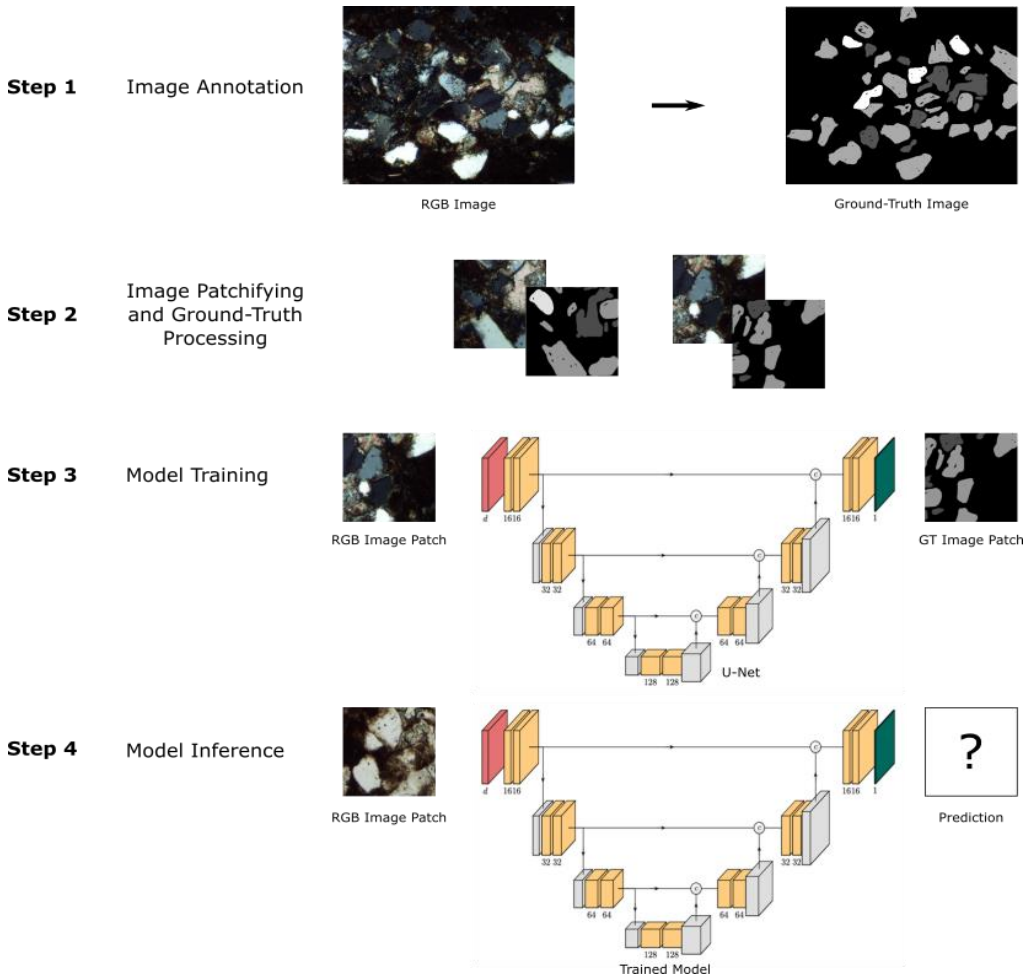

Figure 1. Workflow of U-Net based thin section identification methodology

Database

The present investigation utilized our own database (private) of thin-section rock microscopy images of Mancos shale, a sedimentary rock, taken by a petrographic microscope, with 4 groups. The figure illustrates a series of thin-section images of rocks, displaying the various minerals present within the sections. The database has 993 thin-section images that are captured in color (RGB) format at 10x optical zoom and 300 dpi resolution. The images are 2776×2074 pixels in size and stored in disk with jpeg image format. Figure 2 presents some images from the database.

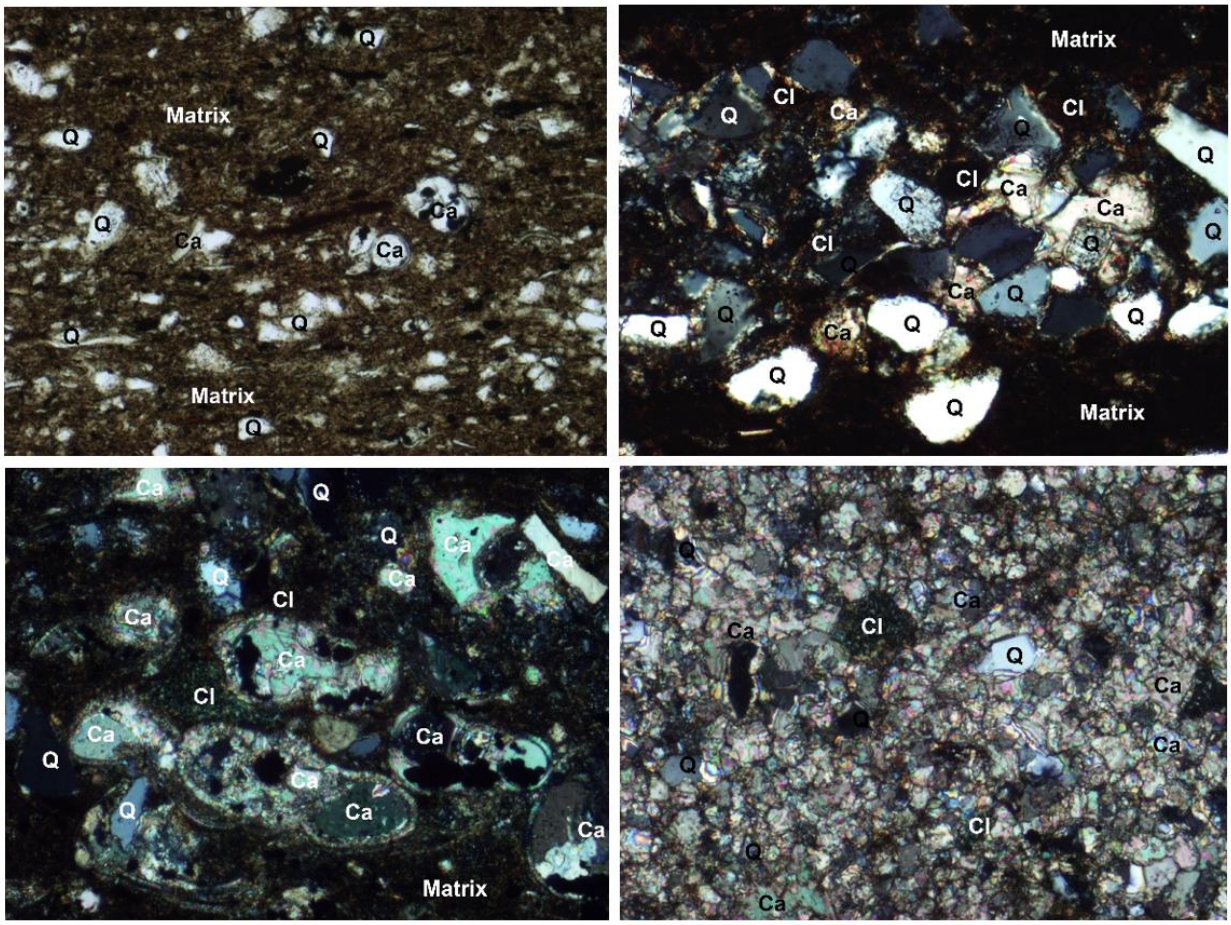

Figure 2. Different types of microscopic thin section images of Mancos Shale with varying minerals (Ca – Calcite, Q – Quartz, Cl- Chlorite, and Matrix). Images are presented with annotated text for better visual purpose.

Dataset Preparation

For training and testing datasets, we carefully select images that are structure-wise and texture-wise different from each other. Afterwards, we randomly sample in 8:2 ratio for the training and validation/test images datasets. Then, we annotate the three types of minerals - calcite, quartz and chlorite, with dark grey, light grey and white colors, respectively, and black for background pixels. The annotations are reviewed with two specialists from the area of image processing and pattern recognition. Afterwards, patches of color thin-section images and their corresponding groud-truth patches are extracted. A total of 320 patches are collected from the training images and 80 patches are collected from the test images. The patch size is 896×896. The location of patches in their corresponding images are sampled randomly so that the distribution of collected patches is not biased to any specific location in the images.

Deep Learning-Based Approach: U-Net

Figure 3 illustrates the vanilla U-Net architecture. Right and left paths are contracting and expanding paths, also known as encoding and decoding units. Both paths are composed of convolutional neural networks. The contraction pathway involves the iterative application of two 3x3 convolutions (which are unpadded convolutions), followed by a rectified linear unit (ReLU) and a 2x2 max pooling operation with a stride of 2 to facilitate down sampling. At each down-sampling stage, the number of feature channels is multiplied by two.

Each stage of the extensive pathway involves an up-sampling of the feature map, which is followed by a 2x2 convolution that reduces the number of feature channels by half. This is then concatenated with the corresponding cropped feature map from the contracting pathway. Finally, two 3x3 convolutions are performed, each followed by a Rectified Linear Unit (ReLU). Each convolution operation results in the loss of border pixels, which requires the need for cropping. The final step in the process involves utilizing a 1x1 convolution to transform the feature vector, which consists of 64 components, into the appropriate number of classes. The model is comprised of a total of 23 convolutional layers.

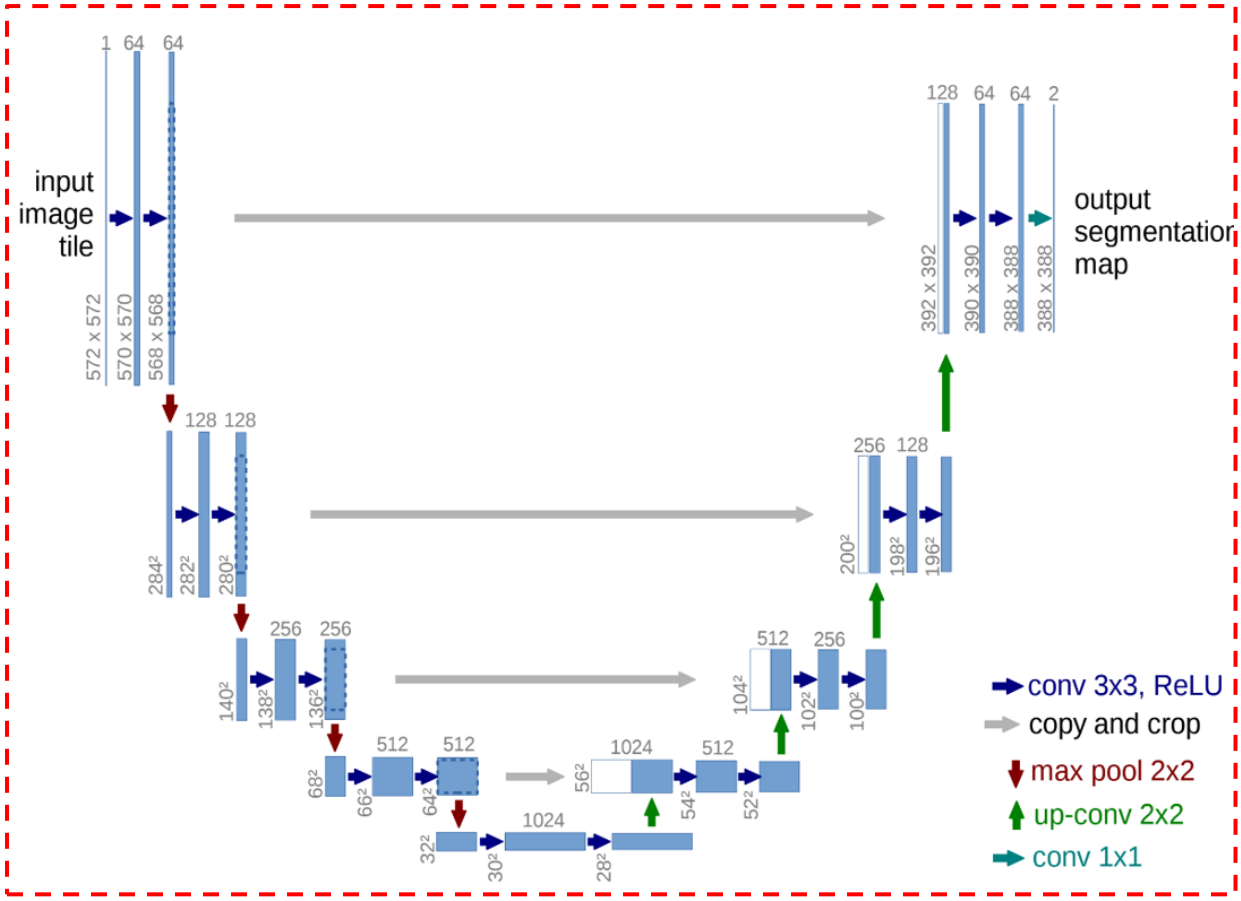

Figure 3. U-Net architecture (vanila). Multi-channel feature maps are blue boxes. Channels are listed on the box. The box's lower left edge shows the x-y-size. White boxes are copied feature maps. (Pattnaik et al. 2020)

The U-Net is a fully convolutional architecture, i.e., the network is composed of convolutional layers only and the input can be of any size. The vanila architecture has 4 layers in the contracting and expanding paths,

with 64, 128, 256 and 512 channels, respectively. The number of layers and channels can be chosen with any preference.

In our experiments, we choose 6 layers with 4, 16, 64, 128, 256 and 512 channels, respectively. The input shape of the model is 896×896×3 and since the model is aimed to classify four classes, the output shape is 896×896×4.

Training

We initialize the weights of network using Kaiming (He et al. 2015) method and fill the biases with 0.01. The weights are optimized with Adam with an initial learning rate of $1\times e^{-4}$, that is reduced by a factor of 0.1 after 10, 120 and 300 epochs using a learning rate scheduler. The training of the network is scheduled by an early stopping criterion with a minimum change in the validation loss of $1\times e^{-7}$and 50 epochs of patience.

We train the model with two different classifiers – i) cross entropy loss and ii) focal loss. Additionally, we consider class-wise weights factors, since the images are inflated with the background class. We apply 0.1 weight for background class, and 0.3 weight for each of the other three classes while computing the loss. The training data is augmented on-fly during training with random vertical flip, random horizontal flip, random 90^0 rotate, random brightness and random contrast normalization.

The model is trained in a GPU-equipped machine that has core-i7-12800HX CPU, NVIDIA GeForce RTX 3070 Ti Mobile GPU with 8GB VRAM, 32 GB RAM and 1TB SSD. The program was written on a Linux Ubuntu 20.04 system using deep learning framework PyTorch.

Model Performance Evaluation Metrices

The performance of the segmentation model can be evaluated qualitatively and quantitatively. Qualitatively, a predicted image is visually inspected and compared with its corresponding the ground-truth image. The texture, shape, edges and position of the predicted objects in the image and the image granularity is observed by visual inspection. For quantitative evaluation, the classification performance is commonly measured using a confusion matrix by distinguishing the positive and negative pixels, as shown in Figure 4. This matrix is obtained by comparing the true and predicted classes. The diagonal elements in the matrix are the number of positive and negative pixels correctly classified as positive and negative, respectively. TP, FN, FP and TN refer to the number of positive pixels correctly classified, number of negative pixels incorrectly classified, number of positive samples incorrectly classified and number of negative samples correctly classified, respectively. Using the data of the confusion matrix, various performance metrics can be computed to evaluate the performance of classifier model.

	Actually Positive (1)	Actually Negative (0)
Predicted Positive (1)	True Positives (TPs)	False Positives (FPs)
Predicted Negative (0)	False Negatives (FNs)	True Negatives (TNs)

Figure 4: Concept of Confusion Matrix

Most commonly the accuracy (ACC), intersection over union (IoU) and f1-score (F1) are used to evaluate the performance of a segmentation model. The computation of the metrices can be performed in two different ways – i) sum the TP, FN, FP and TN pixels over all images and all classes and then compute the metric score, and ii) sum the TP, FN, FP and TN pixels over all images for each class, then compute score for each class separately and then compute the average class scores. The later method does not take class imbalance into account and provides the class-wise average score, while the former approach provides an overall performance score.

Equation (1) and (2) give the formula for computing the accuracy (ACC) and F1-score. According to Figure 4, the IoU is the area of union between the predicted picture and the ground truth image divided by the area of overlap between the two. The IoU metric is considered to be the most useful performance evaluation metric for segmentation model. Using the confusion matrix data, the IoU metric is calculated with equation (3) which is shown in Figure 5.

$$ACC = \frac{TP+TN}{TP+TN+FP+FN} \quad (1)$$

$$F1 = \frac{2TP}{2TP+FP+FN} \quad (2)$$

$$IoU = \frac{TP}{TP+FP+FN} \quad (3)$$

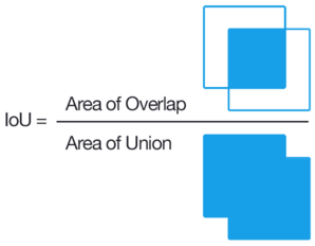

Figure 5: Method to compute IoU for a given predicted and ground-truth images

Results

A few samples of predicted images are shown in Figure 5. We can see some significant amount of false positive pixels in sample 1 and 4. In sample 2, all the classes are notably well classified. The chlorite class is not well detected in all the samples. This illustrates that the characteristics of chlorite class is difficult for the model to learn and there is class-imbalance. Therefore, the dataset needs more accurate annotations and more number of samples which is the part of our future work.

The detailed quantitative results are provided in Table 1. The table shows that the model learns the class variabilities better when trained on focal loss without class weights, that achieved IoU of 0.723. However, the best average IoU per class is 0.298 for the model that is trained with cross entropy loss and weighted class. The overall and class-wise pixel classification accuracy with more than 91% shows that the model is very confident for detecting the classes.

However, the overall measurements are always higher than class-wise measurements for all metrices tells that the background class is influencing the overall measures significantly. To overcome this, the dataset needs to be statistically evaluated for each class balance in order to find the proper weights for the classes.

Additionally, the dataset should include more samples with chlorite class. We recommend these tasks for the future improvement. Figure 7 summarizes the overall accuracy, F1-score, and IoU.

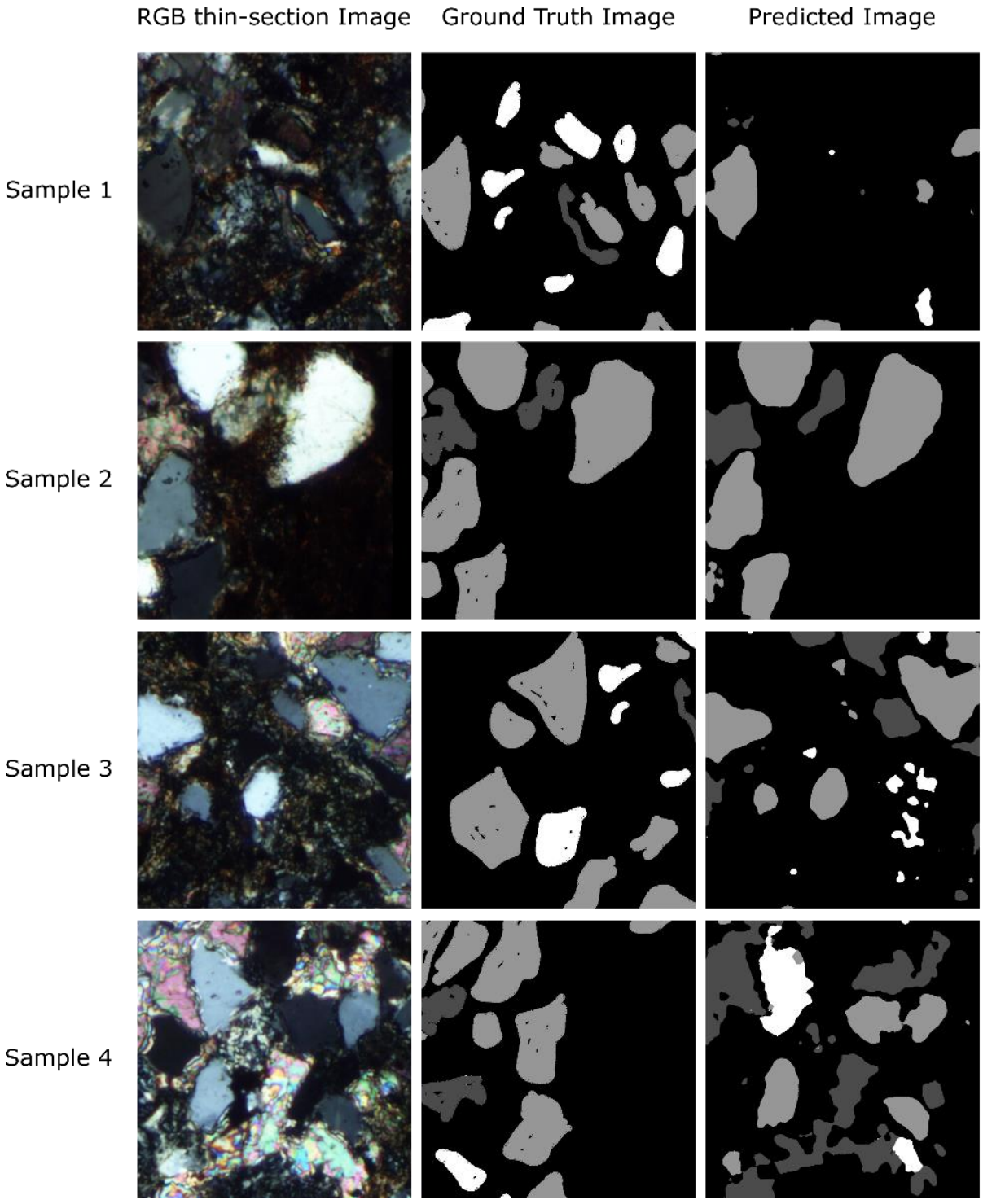

Figure 6. Example of predicted image by the model.

Table 1. The detailed quantitative results

Training Criteria	IoU Overall	IoU Class-wise Average	Accuracy Overall	Accuracy Class-wise Average	F1-Score Overall	F1-Score Class-wise Average
Focal Loss, No weighted class	**0.723**	0.252	**91.9%**	**91.9%**	**0.837**	0.298
Focal Loss, With weighted class	0.719	0.272	91.7%	91.7%	0.835	0.329
Cross Entrophy Loss, No weighted class	0.695	0.288	90.8%	90.8%	0.815	0.365
Cross Entrophy Loss, With weighted class	0.691	**0.298**	90.7%	90.7%	0.815	**0.369**

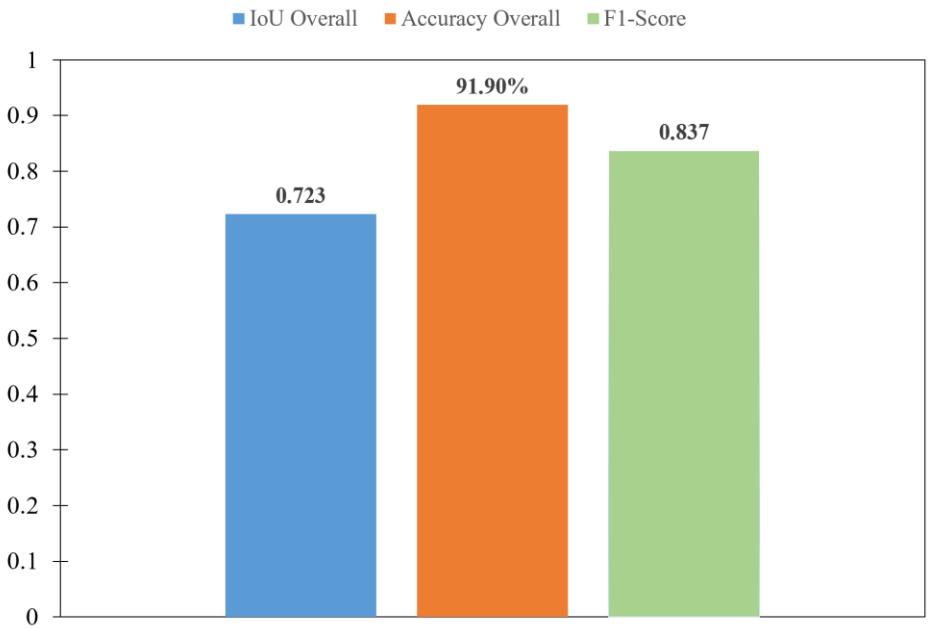

Figure 7. Overall accuracy, F1-score, and IoU

Discussion

This research introduces an intelligent clastic rock thin-section identification technique that improves efficiency and reduces human subjective elements. Geological experts' experience improves intelligent identification accuracy. Compared to intelligent identification, which uses whole-slice samples and artificial intelligence to quantitatively extract information, traditional identification depends on visual observation and local, single-field assessments of the entire.

The U-Net performs well in pixel classification, according to the above experiments. The focal loss and no weighted class training method provides the model most effectiveness for the better categorization of rock thin-section images. When compared to the results of Harinie et al. (2022) (average accuracy 87%) and He et al. (2022) (average precision is 90.89%), our U-Net model classification accuracy for the overall rock minerals is 91.9%. Therefore, this objective we proposed have been shown to be both useful and effective in this application.

There is, however, the opportunity for enhancement in performance. We didn't perform any post-processing on the original photographs before feeding them to the model. Therefore, it may be possible to increase the model's performance by applying a few post-processing techniques to the input image. We experimentally determined that the background class is roughly 85% in each image in our dataset, therefore this high accuracy artificially inflates our overall performance when we have the overall. Creating a well-balanced dataset with high-quality annotation can significantly boost this performance which our future scope of the research.

Conclusions

In this paper, we proposed the U-net architecture to perform the thin section segmentation applications in Mancos shale with varying geological facies. Data augmentation allows to prepare a dataset with annotated ground-truths with calcite, quartz and chlorite objects in thin-section images. Hence, we conducted the pixel-wise classification of calcite, quartz, and chlorite minerals by geological facies and depth from Mancos shale thin-section images using deep learning based supervised model that requires minimal effort to train and test. U-Net demonstrates stable performance with an overall classification precision of 91.90%, F1-scores 0.833, and achieved IoU of 0.723. Optimizer is required for training the supervised U-net network, and the Adam optimizer produced superior results in training the current model. The U-net design can be readily applied to many more jobs. This research trains a high-precision rock thin-section image classification model that may be used to other image classification challenges.

Acknowledgments

The authors would like to thank Texas A&M International University (TAMIU) for supporting the necessary arrangements for this work with a research fund through a TAMIU Presidential Award and University Research Grant (URG).

References

Abedini, M., Ziaii, M., Negahdarzadeh, Y. and Ghiasi-Freez, J., 2018. Porosity classification from thin sections using image analysis and neural networks including shallow and deep learning in Jahrum formation. *Journal of Mining and Environment*, **9**(2), pp.513–525.

Budennyy, S., Pachezhertsev, A., Bukharev, A., et al., 2017. Image processing and machine learning approaches for petrographic thin section analysis (Russian). In: SPE Russian Petroleum Technology Conference. https://doi.org/10.2118/ 187885-MS.

Buono, A., Fullmer, S., Luck, K., et al., 2019. Quantitative digital petrography: full thin section quantification of pore space and grains. In: SPE Middle East Oil and Gas Show and Conference. https://doi.org/10.2118/194899-MS

Cheng, G., Ma, W., & Wei, X. 2013. Rock fabric recognition based on image processing and neural network. Science Technology and Engineering, 28(5), 105-110.

Hu, X.Q., Gao, S.C., Zhang, X., et al., 2012. Rock slice analysis system based on continuous extinction feature analysis. Front. Geosci. 31 (1), 105-110. https://doi.org/10.13745/j.esf.sf.2020.6.36

He, K., Zhang, X., Ren, S. and Sun, J. 2015. Delving Deep into Rectifiers: Surpassing Human-Level Performance on ImageNet Classification. https://doi.org/10.48550/arXiv.1502.01852

Harinie, T.; Janani, C.I.; Sathya, B.S.; Raju, S.; Abhaikumar, V. Classification of rock textures. In Proceedings of the International Conference on Information Systems Design and Intelligent Applications, Visakhapatnam, India, 5–7 January 2012; pp. 887–895.

Jobe, T.D., Vital-Brazil, E. and Khait, M., 2018. Geological feature prediction using image-based machine learning. Petrophysics, 59(06), pp.750–760.

Li, D.; Zhao, J.; Ma, J. 2022. Experimental Studies on Rock Thin-Section Image Classification by Deep Learning-Based Approaches. Mathematics 2022, 10, 2317. https://doi.org/10.3390/math10132317

Ma, Z., Gao, S., 2017. Image analysis of rock thin section based on machine learning. In: International Geophysical Conference, China. https://doi.org/10.1190/igc2017-213.

Nanjo, T., Tanaka, S., 2019. Carbonate lithology identification with machine learning. In: Abu Dhabi International Petroleum Exhibition & Conference. https://doi.org/10.2118/197255-MS.

Pattnaik, S., Chen, S., Helba, A., et al., 2020b. Automatic carbonate rock facies identification with deep learning. SPE Annu. Tech. Conf. Exhib. https://doi.org/10.2118/201673-MS

Pattnaik, S., Chen, S., Shao, W. and Helba, A., 2020a, June. Automating Microfacies Analysis of Petrographic Images. In SPWLA 61st Annual Logging Symposium-Online. Society of Petrophysicists and Well-Log Analysts.

Ronneberger, O., Fischer, P., and Brox, T. 2015. U-Net: Convolutional networks for biomedical image segmentation. In Navab N., Hornegger J., Wells W., Frangi A. (eds) Medical Image

Rubo, R.A., de Carvalho Carneiro, C., Michelon, M.F. and dos Santos Gioria, R., 2019. Digital petrography: Mineralogy and porosity identification using machine learning algorithms in petrographic thin section images. Journal of Petroleum Science and Engineering, 183, p.106382.

Xu, Y., Dai, Z., Luo, Y., 2020. Research on application of image enhancement technology in automatic recognition of rock thin section. IOP Conf. Ser. Earth Environ. Sci. 605 (1), 20e22. https://doi.org/10.1088/1755-1315/605/1/012024.

Zhang, Z., Liu, Q. and Wang, Y., 2018. Road extraction by deep residual u-net. IEEE Geoscience and Remote Sensing Letters, 15(5), pp.749–753.

Zhang, X., Zhang, D., Yang, Z., et al., 2020. Particle segmentation and pore extraction of rock slice based on extinction characteristics of orthogonal polarizing sequence. Acta Petrol. Mineral. 39 (1), 120-128.

Zhou, Z., Rahman Siddiquee, M.M., Tajbakhsh, N., Liang, J. 2018. UNet++: A Nested U-Net Architecture for Medical Image Segmentation. In: , et al. Deep Learning in Medical Image Analysis and Multimodal Learning for Clinical Decision Support. DLMIA ML-CDS 2018 2018. Lecture Notes in Computer Science(), vol 11045. Springer, Cham. https://doi.org/10.1007/978-3-030-00889-5_1